Optimization algorithm performance comparison for hypertrophic cardiomyopathy-modified in-silico cardiomyocytes

Elina Nurkkala[1], Jari Hyttinen[1], Jussi T. Koivumäki[1], Nicole Anderton[1]

[1] Faculty of Medicine and Health Technology, Tampere University, Tampere, Finland

Abstract

As cardiomyocyte models become more complex, efficient optimization algorithms are increasingly important. This study compares the performance and computational cost of the genetic algorithm (GA), particle swarm optimization (PSO), and sailfish optimization (SFO), for calibrating a coupled electro-chemo–mechanical cardiomyocyte model of hypertrophic cardiomyopathy variants with myosin binding protein C mutations c.772G>A (M1) and Gln1061X (M2).

Model parameters were selected based on known mutation-specific effects and a Morris sensitivity analysis. Six contractile parameters were tuned for the six-objective M1 variant, and seven electrophysiological parameters for the three-objective M2 variant. All optimizations stagnated, and 2-100% of Pareto solutions yielded plausible values for over 74% of the assessed physiological biomarkers. GA spacing was 67.9±28.5% and 98.2±4.6% lower than PSO or SFO spacing for M1 and M2, respectively. On average, PSO ran over 20% faster for M2, and SFO 35% faster for M1, with the seed affecting run times significantly. GA showed minor advantage in performance in solution diversity. Thus, careful objective design and parameter selection may have a greater impact on model calibration than the choice of optimization algorithm.

1. Introduction

As computational modeling has become a prominent tool for studying diverse pathophysiologies and drug responses, there is a need for a systematic approach to modify existing complex models to represent disease states and the effects of different mutations [1]. Multiple parameter optimization methods have been developed in the past, and some benchmarking of the these approaches has been conducted in the context of ion channel modeling [2]. Population-based methods are well-suited for multi-objective optimization as they, by design, evaluate multiple points in a parameter space and can provide an estimate of the Pareto front with only a single run [3]. However, no single optimization algorithm performs the best across all problems [3, 4].

In this work, the performance of three population-based metaheuristic algorithms, genetic algorithm (GA), particle swarm optimization (PSO), and sailfish optimization (SFO) are compared in the context of including two novel hypertrophic cardiomyopathy variants caused by MYBPC3-c.772G>A (M1) and MYBPC3-Gln1061X (M2) mutation to a coupled electro-chemo-mechanical cardiomyocyte ODE model. GA, and PSO are well-established algorithms used in multiple fields [5, 6]. To the best of our knowledge, the applicability of more recent SFO to systems biology problems has not previously been evaluated.

2. Methods

Model and parameters: An electro–chemo–mechanical human induced pluripotent stem cell derived cardiomyocyte (hiPSC-CM) model that was calibrated is presented in [7]. Model parameter candidates were selected based on findings from studies conducted on M1 mutated ventricular myocytes and hiPSC-CMs [8, 9], and M2 mutated hiPSC-CMs [10, 11]. Morris method sensitivity analysis was performed to further narrow the selection. For the M1 variant, the chosen parameters were kn_p, kp_n, fapp, gapp, gaslmod, hf, hfmdc, hb and gxb ; all of which are all linked to the rate constants of cross-bridge transitions in the contractile compartment of the model. For the M2 variant, the chosen parameters were cell volume (V_c), membrane capacitance (C_m), conductance of L-type calcium channels (g_{CaL}), conductance of the pacemaker current (g_f), the fraction of g_f attributed to sodium (f_{Na}), and Ca^{2+} disassociation constant of SERCA-pump (kdcai).

Optimization: The `gamultiobj` MATLAB© function was used to perform GA optimization. PSO was based on the method described in [12], and SFO was based on the publicly shared SFO algorithm [13]. Both HCM variants had unique objective functions, based on differences in average biomarker values in [8, 10]. For the M1 variant the optimization targets were: action potential am-

plitude (APA) variation within healthy range, a 65% increase in action potential duration at 50 % repolarization (APD_{50}), a 69% increase in action potential duration at 90 % repolarization (APD_{90}), a 47% increase in time from maximum intracellular calcium to 50% relaxation (CaT RT_{50}), healthy average time from the maximum intracellular calcium to 90% relaxation (CaT RT_{90}), and the time from maximum tension to 50% relaxation (AT RT_{50}) to be higher than the healthy average but lower than the healthy upper limit. For the M2 variant, the targets were a 4% increase in APA, APD_{50} within the healthy range, and a 17% increase in APD_{90}.

Before calculation of the objective function at each fitness evaluation step, the model was run with the modified parameters for 800 s to reach steady state. The model was run in spontaneous mode for both variants, and for the M1 variant, it was also run with 1 Hz pacing, to calculate the contractile element objective. Biomarkers were extracted from 9 APs, CaTs, and tension cycles over the last 30 seconds and compared to the target.

The initial parameter sets had boundaries of 20 % deviation from the original parameter values, and the subsequent iterations allowed ten-fold deviations.All the populations had 100 individuals at the start of the optimization, SFO having 20 sailfish and 80 sardines. Stopping condiitons where a maximum number of iterations was 500 or if the geometric average of the the relative change in the spread was less than 10^{-4} over 100 iterations, and the final value of the spread was less than the mean spread over the last 100 iterations. Each algorithm was executed 10 times, initializing the random number generator with `rng` function, using a seed value corresponding to the run number.

Biomarker evaluation: The final Pareto front estimates of each optimization run were screened based on biomarker values extracted from 9 AP, CaT, and AT cycles over the last 30 seconds of the simulation. From each optimization run, the solutions that met the most biomarker conditions were accepted, with remainder were rejected. For the M1 variant, mutation specific targets were APA and peak intracellular calcium ($Ca_{i,max}$) within 1 % of baseline, active tension amplitude (ATA) higher than baseline, cell shortening less than baseline, and APD_{50}, APD_{90}, CaT duration, CaT RT_{50}, and CaT RT_{90} longer than baseline. For the M2 variant the mutation specific targets were APA and APD_{90} higher than baseline values, resting membrane potential (MDP) and APD_{50} within 1 % of baseline, and $Ca_{i,max}$ and ATA within 50 % of baseline. If not otherwise stated, other evaluated biomarkers were the MDP, peak value of the action potential, action potential cycle length, maximum upstroke velocity, action potential duration at 30 % repolarization, CaT time to peak, CaT rise times from 10 % to 50 and 90 % of the $Ca_{i,max}$, CaT decay time from 90 % to 10 % of $Ca_{i,max}$, CaT duration to 50 % and 90 % decay, diastolic intracellular calcium, ATA, cell shortening %, and AT RT_{50} that were considered acceptable if their values were in healthy range based on [14–17].

Computing environment: In all simulations the system of equations was solved using the ode15s integrator with an initial step size of 2×10^{-5} and a maximum step size of 1.5×10^{-2}. All the optimizations were carried out using MATLAB® (The MathWorks, Inc., Natick, MA, USA) in the computing cluster of Tampere Center for Scientific Computing. Resources requested for the optimizations were 64 GB of memory, 20 CPUs per task, and 13 days of computation time.

3. Results

All the optimization runs stopped owing to reaching the stagnation condition. For M1 optimization, the SFO was significantly faster than GA, and PSO ($p < 0.006$) was over 50% faster on average. No significant differences were observed in run times of GA and PSO for the M1 variant optimization ($p > 0.1$). FOr M2 optimization, PSO was faster than GA and SFO ($p < 0.05$) was over 20% faster on average. There was no significant difference between the run times of GA and SFO ($p > 0.86$). The number of iterations followed the same trend and pattern of statistical significance as the run times. The memory usage was close to 44 GB in all the optimizations for both variants, with no significant difference between algorithms ($p > 0.05$). The number of solutions in the Pareto front estimate were significantly different between the algorithms ($p < 0.02$); SFO having the least solutions along with the widest spread as seen from Figure 1. GA had the lowest median value for the spacing in both optimizations, and the spacing values were significantly lower for GA compared to PSO and SFO in the M2 optimization (two-way ANOVA $p < 0.002$). The number of solutions in the Pareto front estimates, and iterations before terminating, CPU run times, and memory usages are presented in Table 1.

Biomarker-screened Pareto front estimates showed no clear pattern of parameter acceptance. In accepted M1 solutions, the number of biomarkers within the predefined range were, 18 ± 0, 18 ± 1, and 18 ± 1 for GA, PSO, and SFO, respectively. In the M2, the corresponding values were 16 ± 1, 17 ± 1, and 17 ± 2. AP, CaT and AT traces of all Pareto front solutions are presented in Figure 2.

4. Discussion and conclusion

For the M2 optimization, PSO algorithm was the fastest with fewest iterations needed. For the M1 optimization, SFO was the fastest with fewest iterations needed. However, the standard deviations of the run times were high as seen in the Table 1. This suggests that the run times are influenced by the initial values and the initialization of the

Table 1. Number of solutions in Pareto front estimate, number of iterations reached before terminating, memory usage, and CPU run time of MYBPC3-c.772G>A and MYBPC3-Gln1061X optimizations using genetic algorithm (GA), particle swarm optimization (PSO) and sailfish optimization (SFO).

		GA	PSO	SFO
Number of solutions in Pareto front estimate [#]	c.772G>A	35 ± 1	98 ± 5	32 ± 10
	Gln1061X	31 ± 8	17 ± 4	10 ± 4
Last iteration [#]	c.772G>A	156 ± 60	253 ± 178	112 ± 22
	Gln1061X	175 ± 66	121 ± 36	217 ± 124
CPU time [h]	c.772G>A	1925.71 ± 670.73	3232.84 ± 2372.53	945.10 ± 252.02
	Gln1061X	868.94 ± 359.23	536.72 ± 144.01	902.40 ± 440.72
Memory used [GB]	c.772G>A	44.66 ± 0.34	44.44 ± 0.43	44.24 ± 0.24
	Gln1061X	43.78 ± 0.68	43.92 ± 0.83	44.18 ± 0.56

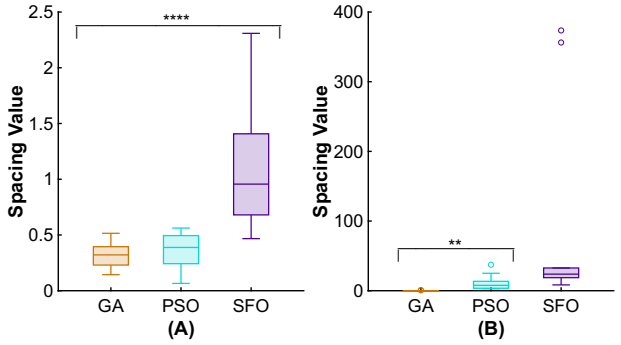

Figure 1. Spacing values of the final Pareto front estimates using genetic algorithm (GA), particle swarm optimization (PSO) and sailfish optimization (SFO) to optimize for (A) MYBPC3-c.772G>A, and (B) MYBPC3-Gln1061X HCM variants. ** Two-way ANOVA p-value < 0.005, **** Two-way ANOVA p-value $< 5 \times 10^{-5}$.

`rng` function. The total combined runtime or the slowest run time is more relevant than individual run times in practice. Repeated optimizations with different seed values might be required, particularly as the outcomes also varied between the runs. Since the required optimization time is typically unknown beforehand [4], and the variation in performance between the algorithms was of a similar magnitude Less iterations used in GA and SFO optimizations of M1 optimization with more objectives compared to M2 may be attributed to the relatively small influence of the parameters on the AP and CaT in the M1 optimization as indicated by Figure 2, despite having optimization targets related to them.

We did not observe significant difference in memory usage, and therefore memory usage cannot be considered a meaningful factor in optimization algorithm choice between GA, PSO and SFO. This may result from inefficient storage of intermediate information, thereby masking differences attributable to the algorithms themselves.

The highest number of Pareto front solutions was obtained with the PSO, and GA algorithms in the M1, and M2 optimization, respectively as seen from Table 1. Although the number of Pareto front solutions is generally expected to be maximized, a Pareto front with fewer solutions may nevertheless outperform one with more solutions [18]. The spacing value is used to evaluate the uniformity of the solutions in the Pareto front, lower values reflecting greater uniformity and considered desirable [18, 19]. GA achieved the lowest median spacing values in both optimizations (Figure 1), but no significant difference was observed compared to PSO in the M1 optimization. The results indicate that solutions of GA Pareto front are more evenly spread.

It is often difficult to determine whether optimization terminates due to local optima, convergence issues, or parameter non-identifiability [4]. The wide range observed in the final Pareto front estimate parameters suggests the presence of at least parameter non-identifiability. As Figure 2 illustrates, there are a large variations in the optimized physiological traces in M2 optimization and active tension of M1 optimization. For the M2 variant, some traces are feasible. Owen et al. compared the performance of optimization algorithms that have been previously applied to ion channel models, and found that the trust region reflective (TRR), as described by Wilhelms et al. [20], performed generally better [2]. However, their study did not incorporate multiple objectives, making these findings not directly applicable in the present context. Additional testing is required to determine whether TRR performs better in this context, and how optimizing algorithm parameters affect the results.

Taken together, GA showed minor advantage in performance in solution diversity compared to PSO and SFO. However, the marginal differences in performance suggest that careful objective design and parameter selection may have a greater impact on model calibration than the choice of optimization algorithm.

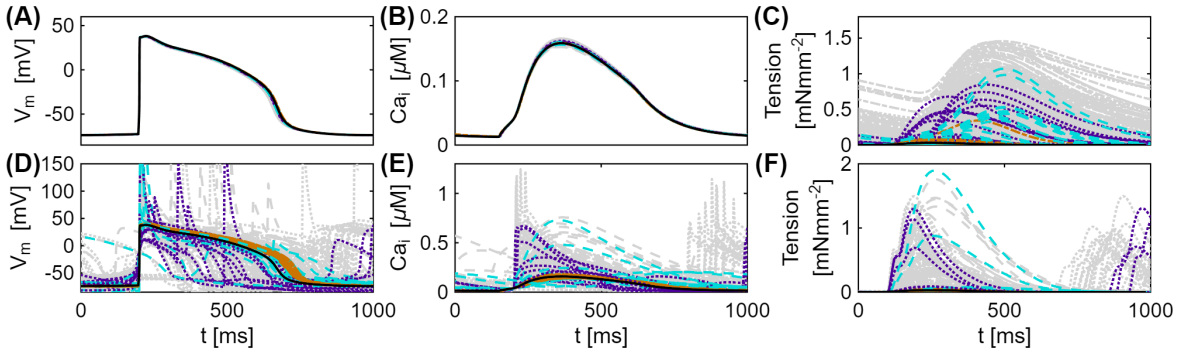

Figure 2. Membrane potential (A & D), intracellular calcium (B & E) and active tension (C & D) traces of genetic algorithm (GA – -), particle swarm optimization (PSO - -), and sailfish optimization (SFO · · ·) solutions that passed the biomarker check in MYBPC3-c.772G>A (A-C) and MYBPC3-Gln1061X (D-F) optimizations. The solutions that were rejected are presented with gray (- -), and the healthy variant trace is presented with black (–).

Acknowledgments

This work is part of the HORIZON-HLTH-2023-TOOL-05 SMASH-HCM project funded by the European Union under Grant 101137115.

References

[1] Yue R, Dutta A. Computational systems biology in disease modeling and control, review and perspectives. NPJ Syst Biol Appl 2022;8(37).

[2] Owen MJ, Mirams GR. IonBench: A benchmark of optimisation strategies for mathematical models of ion channel currents. PLOS Comput Biol 2025;.

[3] Giagkiozis I, et al. An overview of population-based algorithms for multi-objective optimization. Int J Syst Sci 2015; 46:1572–1599.

[4] Kreutz C. Guidelines for benchmarking of optimization-based approaches for fitting mathematical models. Genome Biol 2019;20(281).

[5] Alhijawi B, Awajan A. Genetic algorithms: theory, genetic operators, solutions, and applications. Evol Intell 2024; 17:1245–1256.

[6] Casas-Ordaz A, et al. Particle swarm optmization: A survey of innovations over the last 10 years. Comput Sci Rev 2026; 60(100910).

[7] Forouzandehmehr M, et al. *In silico* study of the mechanisms of hypoxia and contractile dysfunction during ischemia and reperfusion of hiPSC cardiomyocytes. Dis Model Mech 2024;17(dmm050365).

[8] Pioner JM, et al. Slower Calcium Handling Balances Faster Cross-Bridge Cycling in Human *MYBPC3* HCM. Circ Res 2023;132:628–644.

[9] Steczina S, et al. *MYBPC3*-c.772G>A mutation results in haploinsuffiency and altered myosin cycling kinetics in a patient induced stem cell derived cardiomyocyte model of hypertrophic cardiomyopathy. J Mol Cell Cardiol 2024; 191:27–39.

[10] Ojala M, et al. Mutation-Specific Phenotypes in hiPSC-Derived Cardiomyocytes Carrying Either Myosin-Binding Protein C Or α-Tropomyosin Mutation for Hypertrophic Cardiomyopahty. Stem Cells Int 2016;2016(1684792).

[11] Prajapati C, et al. Divergent effects of adrenaline in human induced pluripotent stem cell-derived cardiomyocytes obtained from hypertrophic cardiomyopathy. Dis Model Mech 2018;11(dmm032896).

[12] Shao J, et al. An improved multi-objective particle swarm optimization algorithm for the design of foundation pit of rail transit upper cover project. Sci Rep 2025;15(10403).

[13] Geetha P, et al. Multi-objective DOA estimation in automotive radar using a Sailfish optimizer with Latin hypercube sampling. Soft Comput 2025;29:2433–2461.

[14] Paci M, et al. Automatic Optimization of and *in Silico* Model of Human iPSC Derived Cardiomyocytes Recapitulating Calcium Handling Abnormalities. Front Physiol 2018;9(709).

[15] Paci M, et al. All-Optical Electrophysiology Refines Populations of In Silico Human iPSC-CMs for Drug Evaluation. Biophys J 2020;118:2596–2611.

[16] Margara F, et al. Mechanism based therapies enable personalised treatment of hypertrophic cardiomyopathy. Sci Rep 2022;12(22501).

[17] Mori H, et al. Metabolic remodeling and calcium handling abnormality in induced pluripotent stem cell-derived cardiomyocytes in dialated phase of hypertrophic cardiomyopahty with mybpc3 frameshift mutation. Sci Rep 2024; 14(15422).

[18] Audet C, et al. Performance indicatiors in multiobjective optimization. Eur J Oper Res 2021;292:397–422.

[19] Sharifi MR, et al. A new optimization algorithm to solve multi-objective problems. Sci Rep 2021;11(20326).

[20] Wilhelms M, et al. Calibration of Human Cardiac Ion Current Models to Patch Clamp Measurement Data. Comput Cardiol 2012;39:229–232.

Address for correspondence:

Nicole Anderton, Arvo Ylpön katu 34, 33520, Tampere, Finland, nicole.anderton@tuni.fi